Acta Crystallographica Section A
Foundations of Crystallography
ISSN 0108-7673

Received 24 November 2003
Accepted 22 December 2003

The crystallographic fast Fourier transform. IV. FFT-asymmetric units in the reciprocal space

Andrzej Kudlicki,* Maga Rowicka and Zbyszek Otwinowski

Department of Biochemistry, UT Southwestern Medical Center at Dallas, 5323 Harry Hines Boulevard, Dallas, TX 75390-9038, USA. Correspondence e-mail: andrzej@work.swmed.edu

New algorithms have been outlined for efficient calculation of the fast Fourier transform of data revealing crystallographic symmetries in previous papers by Rowicka, Kudlicki & Otwinowski [*Acta Cryst.* (2002), A**58**, 574–579; *Acta Cryst.* (2003), A**59**, 172–182; *Acta Cryst.* (2003), A**59**, 183–192]. The present paper deals with three implementation-related issues, which have not been discussed before. First, the shape of the FFT-asymmetric unit in the reciprocal space is discussed in detail. Next, a method is presented of reducing symmetry in-place, without the need to allocate memory for intermediate results. Finally, there is a discussion on how the algorithm can be used for the inverse Fourier transform. The results are derived for the case of the one-step symmetry reduction [Rowicka, Kudlicki & Otwinowski (2003). *Acta Cryst.* A**59**, 172–182]. The algorithms are also an important step in the more complicated cases of centered lattices [Rowicka, Kudlicki & Otwinowski (2003). *Acta Cryst.* A**59**, 183–192] and space groups with non-removable special positions, such as cubic groups [Rowicka, Kudlicki & Otwinowski (2004), in preparation]. In the present paper, as in our previous ones, complex-to-complex FFTs only are dealt with. Modifications needed to adapt the results to data with Hermitian symmetry will be described in our forthcoming article [Kudlicki, Rowicka & Otwinowski (2004), in preparation].

1. Background

Algorithms for reducing crystallographic symmetry in fast Fourier transforms for a number of crystallographic space groups have been presented in our previous work (Rowicka *et al.*, 2002, 2003*a*,*b*). These algorithms are based on a novel choice of an asymmetric unit in the real space. Our asymmetric units are regular and retain the periodicity of the crystal. These properties enable us to efficiently reduce the crystallographic symmetry. However, the resulting asymmetric units are non-contiguous. Another innovation is that we are using a non-standard computational grid in the real space. Our grid coordinates are obtained from the fractional coordinates by multiplying them by a matrix **A** and then shifting by a vector **b** (see left panel of Fig. 1). The translation by **b** causes phase shift in the reciprocal space. This affects also groups that do not contain translation in the traditional representation. Additional systematic absences may appear as a result. The asymmetric unit in the real space is defined by the decimation matrix $\mathbf{A}_0$ (see left panel of Fig. 1). The shape of a FFT-asymmetric unit (FFT-ASU) in the reciprocal space depends on the form of the actual symmetry operators and the sizes of grids. Manual design of FFT-ASUs is not feasible. There are many possible choices of FFT-ASU and choosing an appropriate one makes a difference. In Rowicka *et al.* (2002) and Rowicka *et al.* (2003*a*), we have presented specific choices of FFT-ASUs in the reciprocal space for complex-to-complex Fourier transforms in two crystallographic plane groups: *p*3 and *p*4. However, we have not discussed yet how an appropriate FFT-ASU can be chosen for any space group. Designing a procedure for automatic generation of such FFT-ASUs is one of the goals of this paper and is presented in §2. Later, in §5, we will show that, for FFT-ASUs constructed as in §2, our method allows for a fully in-place calculation of the FFT, thus not only reducing the CPU time but also minimizing memory usage. This involves classifying data points according to their

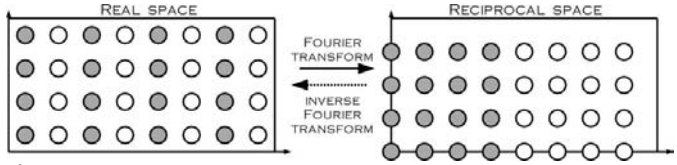

Figure 1
Example of duality between FFT-asymmetric units in the real and reciprocal space for a twofold symmetry and a complex-to-complex Fourier transform. These asymmetric units are defined by the period matrix $\mathbf{A} = \begin{bmatrix} 8 & 0 \\ 0 & 4 \end{bmatrix}$, decimation matrix $\mathbf{A}_0 = \begin{bmatrix} 2 & 0 \\ 0 & 1 \end{bmatrix}$ and a shift vector $\mathbf{b} = \begin{bmatrix} \frac{1}{2} \\ \frac{1}{2} \end{bmatrix}$. Open circles depict grid points not in the asymmetric unit, filled circles are points from the asymmetric unit. Left: FFT-ASU in the real space. Note that the origin of the coordinate system is shifted in the real space. Right: Prototype for a reciprocal-space FFT-asymmetric unit.

algebraic properties, *e.g.* isotropy subgroups (§3). Finally, we will show how the procedure can be applied for calculating the inverse Fourier transform.

We use similar notions and follow the same mathematical notation as in our previous articles and as in Bricogne (1993). In what follows, we recall the most important concepts and symbols. For the reader's convenience, a more thorough mathematical primer is included in Appendix *A*.

Throughout this paper, we will often identify vectors differing by a whole grid. Therefore, we will refer to equivalence classes (see Appendix *A*). The equivalence class of a vector $\mathbf{h}$ with respect to a matrix $\mathbf{B}$ is defined by

$$[\mathbf{h}]_{\mathbf{B}} := \{\mathbf{k} \in \mathbb{Z}^3 : \mathbf{k} - \mathbf{h} \in \mathbf{B}\mathbb{Z}^3\}, \tag{1}$$

where $\mathbb{Z}$ denotes the set of all integers. In this paper, we will use the above construction in two cases. The first one is $[\mathbf{h}]_{\mathbf{A}^T}$, where $\mathbf{A}$ is the matrix defining the crystallographic grid. Then, the reciprocal FFT-unit cell Γ^* is defined as

$$\Gamma^* := \{[\mathbf{h}]_{\mathbf{A}^T} : \mathbf{h} \in \mathbb{Z}^3\}. \tag{2}$$

Note that the number of points in the FFT-unit cell in the reciprocal space is $\det(\mathbf{A}^T) = \det(\mathbf{A})$, that is the same as in the unit cell in the real space. Another example will be used for defining the FFT-ASU prototype in equation (6). Where there is no risk of confusion, we will sometimes write $\mathbf{h}$ instead of $[\mathbf{h}]_{\mathbf{B}}$.

The action of the symmetry operator $S_g = (\mathbf{R}_g, \mathbf{t}_g)$ is given (Bricogne, 1993) in the reciprocal space by

$$S_g^* F(\mathbf{h}) = e_{\mathbf{A}}(\mathbf{h}, \mathbf{t}_g) F(\mathbf{R}_g^T \mathbf{h}), \tag{3}$$

where

$$e_{\mathbf{A}}(\mathbf{h}, \mathbf{t}_g) = \exp(-2\pi i\, \mathbf{h} \cdot \mathbf{A}^{-1} \mathbf{t}_g).$$

2. FFT-asymmetric unit in the reciprocal space

We define the *FFT-asymmetric unit in the reciprocal space* D^* as a subset of a discrete data set Γ^* as follows. First, D^* and its symmetric images should cover the entire FFT-unit cell Γ^*:

$$\bigcup_{g \in G} \bigcup_{\mathbf{h} \in D^*} [\mathbf{R}_g^T \mathbf{h}]_{\mathbf{A}^T} = \Gamma^*. \tag{4}$$

Second, D^* is a minimal subset of the above property. This means that two elements from D^* must not be symmetry-related:

$$\mathbf{h}_1, \mathbf{h}_2 \in D^*, \quad \mathbf{h}_1 \neq \mathbf{h}_2 \Longrightarrow \forall_{g \in G} [\mathbf{R}_g^T \mathbf{h}_1]_{\mathbf{A}^T} \neq \mathbf{h}_2. \tag{5}$$

In other words, all data in a FFT-asymmetric unit are linearly independent. According to the above, the shape of a FFT-asymmetric unit depends on the form of the actual symmetry operators and the sizes of grids. There are many possible choices of FFT-asymmetric unit, we try to choose a convenient one in each case.

In the general case, rather than designing the FFT-asymmetric unit for each group and grid size separately, we generate them automatically, using a heuristic algorithm. The algorithm starts from a prototype Γ_0^*:

$$\Gamma_0^* := \{[\mathbf{h}]_{\mathbf{A}_1^T} : \mathbf{h} \in \mathbb{Z}^3\}, \tag{6}$$

where $\mathbf{A}_1 = \mathbf{A}\mathbf{A}_0^{-1}$. This prototype is dual to the real-space asymmetric unit (see Fig. 1). In particular, it contains the same amount of points as the asymmetric unit in the real space. The FFT-ASU will be derived from Γ_0^* using an iterative routine. The routine works by replacing points in the prototype, thus preserving the total amount of data. First, we identify points in Γ_0^*, which do not belong to a FFT-ASU. Points may be excluded from the FFT-ASU for either of the two following reasons.

(i) Systematic absences, that is points, where the Fourier transform F always equals zero. This happens if, under the action of the symmetry operator $S_g = (\mathbf{R}_g, \mathbf{t}_g)$, the reciprocal-space point $\mathbf{h}$ remains unchanged:

$$[\mathbf{R}_g^T \mathbf{h}]_{\mathbf{A}^T} = \mathbf{h},$$

but the phase of F at this point is shifted by $\varphi := -2\pi \mathbf{h} \cdot \mathbf{A}^{-1} \mathbf{t}_g$, where $\varphi \neq 2k\pi$ (for integer k). In this case, equation (3) reduces to

$$F(\mathbf{h}) = \exp(i\varphi) F(\mathbf{h}), \tag{7}$$

where $\exp(i\varphi) \neq 1$. Then, the only solution is $F(\mathbf{h}) = 0$, regardless of the values of f. Note that the shift of origin in the real space creates non-standard systematic absences in the reciprocal space (see Fig. 3).

(ii) Points whose symmetric images are also in the same prototype of asymmetric unit. These are removed to satisfy (5).

Since the Fourier transform is invertible, the numbers of data points in an asymmetric unit in the real space and in an FFT-asymmetric unit in the reciprocal space must be equal. This means that, for each point removed from the prototype [because of either (i) or (ii) above], an extra point has to be added to it.[1] After the replacement procedure is finished, the modified prototype should satisfy the definition of a FFT-ASU. For reasons that will be explained in §5, we find that good candidates for replacements are points translated by the edges of the initial prototype, $\mathbf{s_0}, \mathbf{s_1}, \mathbf{s_2}$. The algorithm of making the FFT-asymmetric unit is the following:

(i) Set $\mathbf{v}$ to first point from the current prototype. Set FLAG to *false*.

(ii) If $\mathbf{v}$ falls into either of the two categories of points that must be excluded from asymmetric units, then replace $\mathbf{v}$ with $\mathbf{v} + \mathbf{s_0}$ or $\mathbf{v} + \mathbf{s_1}$ or $\mathbf{v} + \mathbf{s_2}$ (at least one of them is always good), and set FLAG to *true*.

(iii) If $\mathbf{v}$ is the last point, and FLAG is *true*, then go to (i).

(iv) Set $\mathbf{v}$ to the next point from the current prototypes, and go to (ii).

The decision, which of the points $\mathbf{v_0} = \mathbf{v} + \mathbf{s_0}$, $\mathbf{v_1} = \mathbf{v} + \mathbf{s_1}$ and $\mathbf{v_2} = \mathbf{v} + \mathbf{s_2}$ to choose in step (ii) of the above algorithm

[1] This is true as long as one considers complex-to-complex Fourier transforms. In a forthcoming paper, we discuss Hermitian symmetry, which may cause points to have fixed phases. Then, two such points carry the same amount of information as one ordinary data point.

requires additional explanation. First, if any of the three is not a valid member of a FFT-asymmetric unit, it is rejected. Next, each of the remaining candidates is assigned a score, the higher the smaller its distance from the prototype. The point with the highest score is selected. In theory, this algorithm may result in infinite loops should some two points compete for a slot near the prototype. A method of exiting such a loop is to change the scoring function. There are many good choices of a new score, *e.g.* reverse of the original, or even a random score. The freedom of choosing a new score does not mean that the asymmetric unit will change between calculations. Once a FFT-ASU shape is generated for a set of grid parameters and symmetry operators, it can be saved and re-used every time the FFT routine is called with these parameters.

A schematic flow chart of making FFT-ASUs from prototypes is presented in Fig. 2. In Fig. 3, we present an example of the difference between the FFT-ASU and its prototype.

The algorithms presented in this section produce a FFT-ASU, on which the Fourier transform will be calculated. This FFT-ASU is as compact and as regular as possible, which will prove to be important in the process of the actual computations.

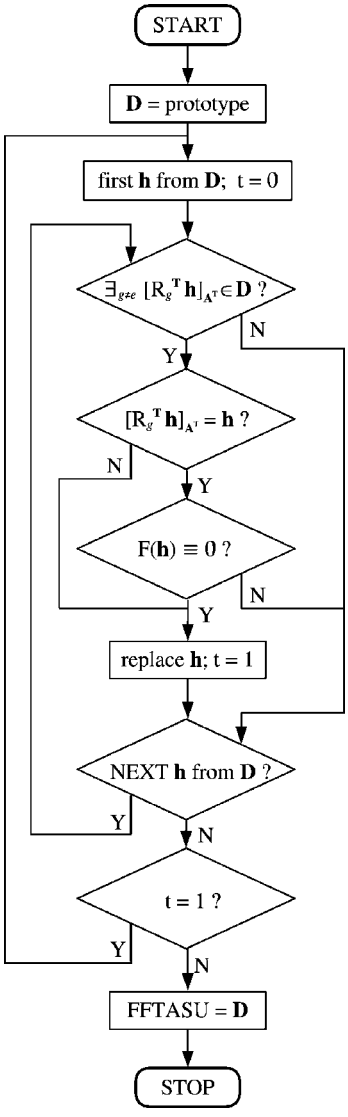

Figure 2
A flow chart of the algorithm for iterating FFT-ASU prototypes. The main (inner) loop is performed over all points in the prototype of the FFT-asymmetric unit. This entire loop is repeated until the current prototype **D** is a valid FFT-ASU (outer loop). This is the case when no point replacements in **D** have been made during the last cycle of the outer loop, *i.e.* $t = 0$. The symbol e denotes the identity operator in the group G. Points are replaced as described in §2.

3. Isotropy subgroups and their related quotient groups

The next step after specifying the FFT-ASU is to classify its points with respect to their properties relevant in the subsequent calculations. The most obvious of such properties is the isotropy subgroup of the point in question. We define the isotropy subgroup of a point $\mathbf{h}$ in the reciprocal space $G_{\mathbf{h}}$ as a set of those operators from the underlying crystallographic group G whose rotational parts transform $\mathbf{h}$ onto itself:

$$G_{\mathbf{h}} = \{g \in G : [\mathbf{R}_g^T \mathbf{h}]_{\mathbf{A}^T} = \mathbf{h}\}. \quad (8)$$

Note that $G_{\mathbf{h}}$ is indeed a subgroup of G. Moreover, every subgroup of G may be an isotropy subgroup of a point. The smallest possible isotropy subgroup consists only of the identity element e. The biggest is the whole group G. The number of elements of the isotropy group will be called the *multiplicity* of the point $\mathbf{h}$.

Another useful notion is that of a quotient group $G/G_{\mathbf{h}}$. The group $G/G_{\mathbf{h}}$ is a set of distinct cosets

$$gG_{\mathbf{h}} = \{gu : u \in G_{\mathbf{h}}\}.$$

The *orbit* $G\mathbf{h}$ of a point $\mathbf{h}$ is the collection of all distinct images of $\mathbf{h}$ under the action of group G. The number of elements of the orbit of a point $\mathbf{h}$ coincides with the number of elements of the quotient group $G/G_{\mathbf{h}}$. Note that

$$|G| = |G_{\mathbf{h}}||G/G_{\mathbf{h}}| = |G_{\mathbf{h}}||G\mathbf{h}| = \text{multiplicity}(\mathbf{h})|G\mathbf{h}|, \quad (9)$$

where $|G|$ denotes the number of elements of G *etc.* A simple example explaining the notions introduced above is presented in Fig. 4. However, this example does not cover all the phenomena arising in our considerations. In particular, in some cases two points $\mathbf{h}_1$ and $\mathbf{h}_2$ with different isotropy subgroups $G_{\mathbf{h}_1} \neq G_{\mathbf{h}_2}$ may still yield the same quotient group $G/G_{\mathbf{h}_1} = G/G_{\mathbf{h}_2}$. For a practical example, let us consider the space group $P422$. Let the FFT-unit cell be given by

$$\Gamma^* = \{0, 1, \ldots, 7\} \times \{0, 1, \ldots, 7\} \times \{0, 1\}.$$

The rotational parts of the symmetry operators in the grid coordinate system are the same as in the crystallographic (fractional) coordinates:

$$\mathbf{R}_1 = \begin{bmatrix} 1 & 0 & 0 \\ 0 & 1 & 0 \\ 0 & 0 & 1 \end{bmatrix} \quad \mathbf{R}_2 = \begin{bmatrix} -1 & 0 & 0 \\ 0 & 1 & 0 \\ 0 & 0 & -1 \end{bmatrix}$$

$$\mathbf{R}_3 = \begin{bmatrix} -1 & 0 & 0 \\ 0 & -1 & 0 \\ 0 & 0 & 1 \end{bmatrix} \quad \mathbf{R}_4 = \begin{bmatrix} 1 & 0 & 0 \\ 0 & -1 & 0 \\ 0 & 0 & -1 \end{bmatrix}$$

$$\mathbf{R}_5 = \begin{bmatrix} 0 & -1 & 0 \\ 1 & 0 & 0 \\ 0 & 0 & 1 \end{bmatrix} \quad \mathbf{R}_6 = \begin{bmatrix} 0 & 1 & 0 \\ 1 & 0 & 0 \\ 0 & 0 & -1 \end{bmatrix}$$

$$\mathbf{R}_7 = \begin{bmatrix} 0 & 1 & 0 \\ -1 & 0 & 0 \\ 0 & 0 & 1 \end{bmatrix} \quad \mathbf{R}_8 = \begin{bmatrix} 0 & -1 & 0 \\ -1 & 0 & 0 \\ 0 & 0 & -1 \end{bmatrix}.$$

The isotropy subgroups of points $\mathbf{h}_1 = [1, 0, 0]$ and $\mathbf{h}_2 = [0, 1, 0]$ are the following:

$$G_{\mathbf{h}_1} = \{\mathbf{R}_1^T, \mathbf{R}_2^T\}, \quad G_{\mathbf{h}_2} = \{\mathbf{R}_1^T, \mathbf{R}_4^T\}.$$

Clearly,

$$G_{\mathbf{h}_1} \neq G_{\mathbf{h}_2},$$

nonetheless their corresponding quotient groups coincide:

$$G/G_{\mathbf{h}_1} = \{\mathbf{R}_1^T, \mathbf{R}_3^T, \mathbf{R}_5^T, \mathbf{R}_7^T\} = G/G_{\mathbf{h}_2}.$$

4. Implications of the symmetry-reduction formula

The core of crystallographic FFT computation is the implementation of the symmetry-reduction formula (Rowicka *et al.*, 2003*a*). For points from the prototype Γ_0^*, it has the following simple form:

$$F(\mathbf{h}) = \sum_{g \in G} e_{\mathbf{A}}(\mathbf{h}, \mathbf{t}_g) Y([\mathbf{R}_g^T \mathbf{h}]_{A_1^T}), \tag{10}$$

where Y is the Fourier transform of data from the real-space asymmetric unit Γ_0:

$$Y(\mathbf{h}) = \sum_{\gamma \in \Gamma_0} f(\gamma) e_{\mathbf{A}}(\mathbf{h}, \gamma). \tag{11}$$

Note that the sum in equation (10) is over the points from the orbit of $\mathbf{h}$. Should the multiplicity of $\mathbf{h}$ be greater than one, some of these points are repeated with different phase factors. In this case, the orbit has fewer distinct elements than $|G|$ [*cf.* equation (9)].

As we have shown in §2, the actual FFT-ASU may not coincide with its prototype. It usually differs from the prototype by a few points. The points from Γ_0 that do not belong to the FFT-ASU are replaced by points translated by an edge of the prototype, $\mathbf{s}_i$. Let us see what is the impact of replacing $\mathbf{h}_1$ by $\mathbf{h}_1 + \mathbf{s}_i$ on the symmetry reduction:

$$F(\mathbf{h}_1 + \mathbf{s}_i) = \sum_{g \in G} e_{\mathbf{A}}(\mathbf{s}_i, \mathbf{t}_g) e_{\mathbf{A}}(\mathbf{h}_1, \mathbf{t}_g) Y([\mathbf{R}_g^T (\mathbf{h}_1 + \mathbf{s}_i)]_{A_1^T}).$$

Note that since $\mathbf{s}_i$ is a prototype edge and $[\cdot]_{\mathbf{A}_1^T}$ denotes coordinates taken modulo prototype, then

$$[\mathbf{R}_g^T (\mathbf{h}_1 + \mathbf{s}_i)]_{\mathbf{A}_1^T} = [\mathbf{R}_g^T \mathbf{h}_1]_{\mathbf{A}_1^T}.$$

From the above,

$$F(\mathbf{h}_1 + \mathbf{s}_i) = \sum_{g \in G} e_{\mathbf{A}}(\mathbf{s}_i, \mathbf{t}_g) \{e_{\mathbf{A}}(\mathbf{h}_1, \mathbf{t}_g) Y([\mathbf{R}_g^T \mathbf{h}_1]_{A_1^T})\}. \tag{12}$$

The right-hand sides of (10) and (12) differ only by the factor $e_{\mathbf{A}}(\mathbf{h}_1, \mathbf{t}_g)$ under the sum. Replacing points by their translation by $\mathbf{s}_i$ introduces only a slight modification to the symmetry-reduction formula. Also, the orbits of the points taken modulo prototype remain unchanged. This is our motivation for choosing the replacement procedure proposed in §2.

5. In-place forward and inverse FFT

In this section, we will show how the form of the symmetry reduction formula [(10) and (12)] allows one to perform the symmetric part of the FFT calculation (computing F from Y) in-place. First, note that in order to compute $F(\mathbf{h})$ the only points at which Y need be known are the ones from the orbit of $\mathbf{h}$ (modulo prototype). Also, these data are also sufficient to evaluate the Fourier transform F on the whole orbit of $\mathbf{h}$ (again modulo prototype). This property is crucial because it enables us to compute F from Y 'orbit by orbit'. In particular, after processing an orbit, we can store the resulting F's in the same memory addresses we have taken the Y's from.

The Fourier transform is a linear operation and so is its symmetric part. Hence, for the orbit of a point $\mathbf{h}$, the symmetric step can be represented by multiplication by a square $|G/G_{\mathbf{h}}| \times |G/G_{\mathbf{h}}|$ matrix (see Fig. 5). Let us call this matrix $\mathbf{M}_{\mathbf{h}}$. Its entries are given by the symmetry reduction formula

$$F(\mathbf{R}_{g_p}^T \mathbf{h}) = \sum_q e_{\mathbf{A}}^T(\mathbf{R}_{g_p}^T \mathbf{h}, \mathbf{t}_{g_q^{-1}}) Y(\mathbf{R}_{g_q^{-1}}^T \mathbf{R}_{g_p}^T \mathbf{h}).$$

The multiplication table in G has to be pre-computed in order to obtain entries of the matrix $\mathbf{M}_{\mathbf{h}}$. In the simplest case, when all points from the orbit of the point $\mathbf{h}$ have trivial isotropy subgroups (*i.e.* multiplicity 1), then $\mathbf{M}_{\mathbf{h}}$ is a $|G| \times |G|$ matrix and all its entries have modulus 1.

If $\mathbf{h}$ has a nontrivial isotropy subgroup $G_{\mathbf{h}}$ with $m_{\mathbf{h}}$ elements, then $\mathbf{M}_{\mathbf{h}}$ has a slightly more complicated structure. Namely, it is a product of a matrix $\mathbf{M}_{\mathbf{h}}^0$ with entries of modulus 1, times a diagonal matrix $\mathbf{D}_{\mathbf{h}}$, with diagonal entries being a sum of $m_{\mathbf{h}}$ appropriate twiddle factors:

$$\mathbf{M}_{\mathbf{h}} = \mathbf{M}_{\mathbf{h}}^0 \mathbf{D}_{\mathbf{h}}.$$

The matrix $\mathbf{D}_{\mathbf{h}}$ has the following form:

$$\mathbf{D}_{\mathbf{h}} = \begin{bmatrix} \sum_{l=1}^{m_{\mathbf{h}}} \exp(i\varphi_{l,1}) & 0 & \dots & 0 \\ 0 & \sum_{l=1}^{m_{\mathbf{h}}} \exp(i\varphi_{l,2}) & \dots & 0 \\ \vdots & \vdots & & \vdots \\ 0 & 0 & \dots & \sum_{l=1}^{m_{\mathbf{h}}} \exp(i\varphi_{l,|G|/m_{\mathbf{h}}}) \end{bmatrix},$$

where $\varphi_{l,n}$ denote the appropriate phase shifts, as in equation (12). Let $\mathbf{M}$ denote a block-diagonal matrix, consisting of the matrices $\mathbf{M}_{\mathbf{h}}$, numbered by representatives of all distinct orbits in the FFT-ASU:

$$\mathbf{M} = \bigoplus_{G\mathbf{h}} \mathbf{M}_{\mathbf{h}} = \begin{bmatrix} \mathbf{M}_{\mathbf{h}_1} & 0 & \dots & 0 \\ 0 & \mathbf{M}_{\mathbf{h}_2} & \dots & 0 \\ \vdots & \vdots & & \vdots \\ 0 & 0 & \dots & \mathbf{M}_{\mathbf{h}_k} \end{bmatrix},$$

where k is the number of distinct orbits. For each $\mathbf{h}$, the matrix $\mathbf{M}_{\mathbf{h}_i}$ has the dimensions $(|G|/m_{\mathbf{h}}) \times (|G|/m_{\mathbf{h}})$, whose possible values in one-step symmetry reduction are 1×1, 2×2, 3×3, 4×4, 6×6 or 8×8.

Calculating the Fourier transform in the FFT-asymmetric unit, $F_{|\mathrm{ASU}}$, from the real-space asymmetric unit data, $f_{|\mathrm{ASU}}$, can be represented by multiplication by a matrix:

$$F_{|\mathrm{ASU}} = \mathbf{F}_{|\mathrm{ASU}} f_{|\mathrm{ASU}}.$$

Our method of calculating $F_{|\mathrm{ASU}}$ can be thought of as consisting of three steps. Each of these steps can be expressed by a matrix multiplication. First, we apply the $P1$ Fourier transform matrix $\mathbf{Y}$ to the real-space asymmetric unit data $f_{|\mathrm{ASU}}$. Next, a permutation matrix $\mathbf{P}$ aligns orbits of points together. Finally, the symmetric part of the FFT can be represented by a block-diagonal matrix $\mathbf{M}$, with appropriate matrices $\mathbf{M}_{\mathbf{h}}$ on its diagonal:

$$\mathbf{F}_{|\mathrm{ASU}} = \mathbf{MPY}. \tag{13}$$

Now that we have reduced $\mathbf{F}_{|\mathrm{ASU}}$ to this form, the inverse Fourier transform reads:

$$\mathbf{F}^{-1}_{|\mathrm{ASU}} = \mathbf{Y}^{-1}\mathbf{P}^{-1}\mathbf{M}^{-1}.$$

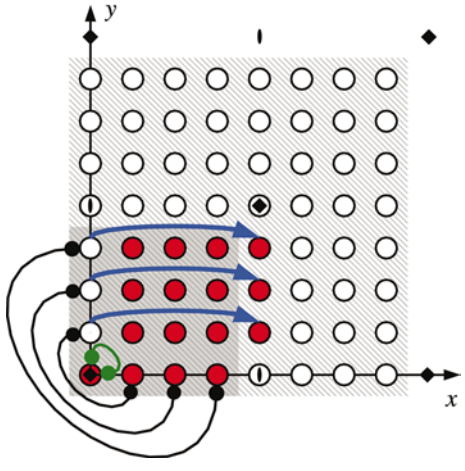

Figure 3
Differences between a FFT-ASU and its prototype. The symmetry group is the planar group $p4$. Circles in the dashed area depict the FFT-unit cell. The symmetry operator symbols in the figure depict operators, containing additional phase shifts due to the non-standard origin of the coordinates in the real space. The prototype of the FFT-ASU consists of the points in the shaded area. Connectors with circles correspond to symmetry action within the prototype. Black connectors depict disqualifying symmetry, while the green connector shows a point with higher multiplicity (non-disqualifying symmetry). Points disqualified from the prototype are replaced with points translated by the edge of the prototype, as shown by blue arrows. The resulting FFT-ASU is colored red. The points [0,4], [4,0] and [4,4] are the systematic absences, so they do not belong to any image of the FFT-ASU.

$\mathbf{M}$, being a block-diagonal matrix, can be inverted easily. The calculation reduces to inverting the small matrices $\mathbf{M}_{\mathbf{h}}$:

$$\mathbf{M}^{-1} = \bigoplus_{G\mathbf{h}} \mathbf{M}^{-1}_{\mathbf{h}},$$

Clearly, the inverse of the permutation matrix is its transposition, $\mathbf{P}^{-1} = \mathbf{P}^{T}$ (see *e.g.* Tolimieri *et al.*, 1997). The final step, applying $\mathbf{Y}^{-1}$, is in practice performed by P1-FFT library functions (using the Cooley–Tukey decomposition). This completes the description of performing both forward and inverse FFT in-place.

6. Discussion

We have discussed the shapes of FFT-asymmetric units in the reciprocal space for complex-to-complex crystallographic FFTs. In crystallography, Fourier transforms are real-to-

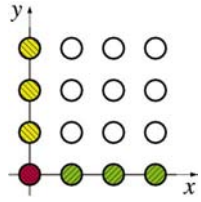

Figure 4
Isotropy subgroups in the case of the planar group $G = Pmm$. This group consists of four operators: $e = (x, y)$, $g_1 = (-x, y)$, $g_2 = (x, -y)$ and $g_3 = (-x, -y)$. The points on the x axis (green, $\mathbf{h}_x = [x, 0]$) are invariant with respect to e and g_2. Therefore, these points have multiplicity 2 and their isotropy subgroup is $G_{[x,0]} = \{e, g_2\}$. Their corresponding quotient group $G/G_{[x,0]}$ consists of two elements: $G/G_{[x,0]} = \{e, g_1\}$. Both g_1 and g_2 are involutions, so $G_{[x,0]}$ and $G/G_{[x,0]}$ are indeed groups. Analogously, points on the y axis (yellow, $\mathbf{h}_y = [0, y]$) have multiplicity 2, the isotropy subgroup $G_{[0,y]} = \{e, g_1\}$ and the corresponding quotient group $G/G_{[0,y]} = \{e, g_2\}$. The point [0, 0] (red) is invariant with respect to all operators from G, so $G_{[0,0]} = G$, while the quotient group is trivial: $G/G_{[0,0]} = \{e\}$. The multiplicity of the point [0, 0] equals 4. All other points (white) are invariant only with respect to e, so they have multiplicity 1, trivial isotropy subgroup, and their quotient group is the whole G. Here, we assumed there are more than eight points along all the unit-cell edges. Therefore, the other point with non-trivial isotropy subgroup, which lies exactly at the middle of the unit cell, is not shown in this figure.

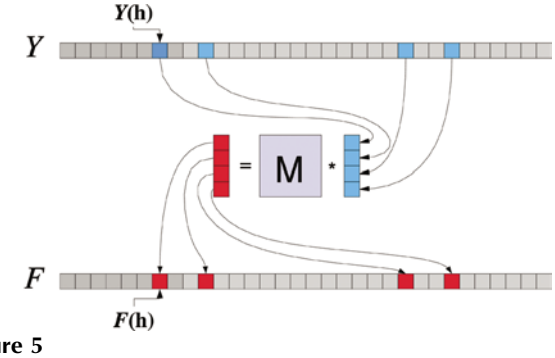

Figure 5
Schematic illustration of the method of obtaining the values of the Fourier transform F on the orbit of $\mathbf{h}$ (red) from the values of Y at the same set of points (blue). This is done through a multiplication by a matrix $\mathbf{M}$. This calculation is done fully in-place.

complex or complex-to-real transforms. To perform efficiently real-to-complex FFT calculations, one encodes two real numbers as one complex number. This procedure is called multiplexing. After multiplexing, a complex-to-complex FFT is performed. In the present article, we have described an efficient FFT-ASU choice for complex-to-complex crystallographic FFT. Designing a multiplexing compatible with crystallographic symmetry is a separate problem. Optimal multiplexing should be performed fully in-place. Doing multiplexing fully in-place is a difficult task even if there is no crystallographic symmetry involved. The shapes of 3D asymmetric units due to Hermitian symmetry only are inherently quite complicated; this is why they are not implemented in standard FFT libraries such as *FFTW* (Frigo & Johnson, 1998) or *Numerical Recipes* (Press *et al.*, 1992) (additional data arrays in the reciprocal space are allocated in these programs). Our approach allows for combining Hermitian and crystallographic symmetry, while performing all the calculations fully in-place. The details of our solution are beyond the scope of this article, and they are presented in our next paper (Kudlicki *et al.*, 2004).

APPENDIX *A*
Mathematical notions and notation

Let $\mathbb{Z}$ denote the set of all integers and $\mathbb{Z}^3$ denote the Cartesian product $\mathbb{Z}\times\mathbb{Z}\times\mathbb{Z}$. Matrices and vectors will be written in bold type. The standard basis vectors of $\mathbb{Z}^3$ will be denoted by $\mathbf{e}_1$, $\mathbf{e}_2$ and $\mathbf{e}_3$. Our goal is to compute discrete Fourier transforms of a periodic function f defined on $\mathbb{Z}^3$. Such a function will have the periodicity of the underlying crystal structure, described by a 3×3 matrix with integer entries, $\mathbf{A}$. From now on, we will require that $\mathbf{A}$ be invertible (that is, that its determinant is not equal to zero: $\det\mathbf{A}\neq 0$). The periodicity condition reads

$$f(\mathbf{x}+\mathbf{t})=f(\mathbf{x}),$$

where $\mathbf{x}\in\mathbb{Z}^3$ and

$$\mathbf{t}\in\mathbf{A}\mathbb{Z}^3=\{\mathbf{x}\in\mathbb{Z}^3:\ \text{there exists a } \mathbf{y}\in\mathbb{Z}^3 \text{ such that } \mathbf{x}=\mathbf{A}\mathbf{y}\}.$$

We use the notion of an *equivalence relation*, a useful example of which is given by

$$\mathbf{y}\,\mathcal{R}_{\mathbf{A}}\,\mathbf{x}\Leftrightarrow\mathbf{y}-\mathbf{x}\in\mathbf{A}\mathbb{Z}^3.$$

This means that $\mathbf{x}$ and $\mathbf{y}$ are in the relation $\mathcal{R}_{\mathbf{A}}$ if and only if they have the same fractional coordinates. The equivalence class of $\mathbf{x}$ (with respect to the relation $\mathcal{R}_{\mathbf{A}}$) will be

$$[\mathbf{x}]_{\mathbf{A}}=\{\mathbf{y}\in\mathbb{Z}^3\ :\ \mathbf{y}-\mathbf{x}\in\mathbf{A}\mathbb{Z}^3\}.$$

Another useful notion will be that of a *quotient space* (see also Rowicka *et al.*, 2003*a*; Bricogne, 1993). In this article, we deal with the quotient space of $\mathbb{Z}^3$ by $\mathbf{A}\mathbb{Z}^3$

$$\mathbb{Z}^3/\mathbf{A}\mathbb{Z}^3=\{[\mathbf{x}]_{\mathbf{A}}:\mathbf{x}\in\mathbb{Z}^3\}.$$

The notion of a quotient space allows us to describe periodicity conditions in a very convenient way. Instead of viewing f as a periodic function, it can be equivalently considered as defined on the set of the equivalence classes $\mathbb{Z}^3/\mathbf{A}\mathbb{Z}^3$. Let us introduce the notation

$$\Gamma=\mathbb{Z}^3/\mathbf{A}\mathbb{Z}^3 \tag{14}$$

and

$$\Gamma^*=\mathbb{Z}^3/\mathbf{A}^T\mathbb{Z}^3,$$

where $\mathbf{A}^T$ denotes the transposition of matrix $\mathbf{A}$. The space Γ^* is a space dual to Γ. Its elements are covectors, *i.e.* objects dual to vectors (for more details see Rowicka *et al.*, 2004*b*). Covectors are printed in bold type and they will be, when there is no risk of confusion, also referred to as vectors. The scalar product of a covector $\mathbf{h}\in\Gamma^*$ and a vector $\mathbf{x}\in\Gamma$, expressed in standard bases, reads

$$\mathbf{h}\cdot\mathbf{x}=(h\mathbf{e}_1^*+k\mathbf{e}_2^*+l\mathbf{e}_3^*)\cdot(x\mathbf{e}_1+y\mathbf{e}_2+z\mathbf{e}_3)=hx+ky+lz,$$

where $h, k, l, x, y, z\in\mathbb{Z}$. We use a shorthand notation $e_{\mathbf{A}}(\mathbf{h},\mathbf{x})$ for the coefficient (also called 'twiddle factor') occurring frequently throughout this paper

$$e_{\mathbf{A}}(\mathbf{h},\mathbf{x})=\exp(-2\pi i\,\mathbf{h}\cdot\mathbf{A}^{-1}\mathbf{x}).$$

This symbol has the following properties:

$$e_{\mathbf{A}}(\mathbf{g}+\mathbf{h},\mathbf{x})=e_{\mathbf{A}}(\mathbf{g},\mathbf{x})e_{\mathbf{A}}(\mathbf{h},\mathbf{x})$$
$$e_{\mathbf{A}}(\mathbf{h},\mathbf{x}+\mathbf{y})=e_{\mathbf{A}}(\mathbf{h},\mathbf{x})e_{\mathbf{A}}(\mathbf{h},\mathbf{y})$$

for any $\mathbf{g},\mathbf{h}\in\Gamma^*$ and $\mathbf{x},\mathbf{y}\in\Gamma$. Let f be a complex-valued function on Γ, where Γ is given by equation (14). The Fourier transform of function f is denoted by F and for any $\mathbf{h}\in\Gamma^*$ defined by

$$F(\mathbf{h})=\sum_{\mathbf{x}\in\Gamma}f(\mathbf{x})e_{\mathbf{A}}(\mathbf{h},\mathbf{x}). \tag{15}$$

For simplicity, in the above formula, we have omitted the normalization constant $1/|\det\mathbf{A}|$.

A1. Crystallographic group action

Let G denote the quotient (or factor) crystallographic space group (Bricogne, 1993; Rowicka *et al.*, 2003*a*). The elements of G are the symmetry operators as listed in *International Tables for Crystallography* (Hahn, 1995). The group operation in G is the ordinary composition of symmetry operators. We represent the action of an element $g\in G$ in the real space as follows:

$$S_g(\mathbf{x})=\mathbf{R}_g\mathbf{x}+\mathbf{t}_g, \tag{16}$$

where $\mathbf{x}\in\Gamma$. We call $\mathbf{R}_g$ the rotational part of the symmetry operator related to g. Since $\det\mathbf{R}_g=\pm1$, it follows that $\mathbf{R}_g$ can be either a proper ($\det\mathbf{R}_g=1$) or an improper ($\det\mathbf{R}_g=-1$) rotation. We call $\mathbf{t}_g$ a translational part of the symmetry operator. We stress that, since $\mathbf{x}\in\Gamma=\mathbb{Z}^3/\mathbf{A}\mathbb{Z}^3$, the symbol $\mathbf{x}$ in the formula above is in fact the equivalence class $[\mathbf{x}]_{\mathbf{A}}$. The action (16) defines an action $S^{\#}$ on a function f in space Γ by

$$(S_g^{\#}f)(\mathbf{x})=f(S_g^{-1}(\mathbf{x}))=f(\mathbf{R}_g^{-1}(\mathbf{x}-\mathbf{t}_g)).$$

This action $S^{\#}$ on the functions in the real space extends to the action S^{*} on their Fourier transforms in the reciprocal space,

$$S_g^* F(\mathbf{h}) = e_{\mathbf{A}}(\mathbf{h}, \mathbf{t}_g) F(\mathbf{R}_g^T \mathbf{h}). \quad (17)$$

The research was supported by grant NIH GM 53163. We thank the referee for useful comments.

References

Bricogne, G. (1993). In *International Tables for Crystallography*, Vol. B, edited by U. Shmueli. Dordrecht: Kluwer Academic Publishers.
Frigo, M. & Johnson, S. (1998). Proc. 1998 IEEE International Conference on Acoustics, Speech, and Signal Processing, pp. 1381–1384.
Hahn, T. (1995). Editor. *International Tables for Crystallography*, Vol. A. Dordrecht: Kluwer Academic Publishers.
Kudlicki, A., Rowicka, M. & Otwinowski, Z. (2004). In preparation.
Press, W. H., Teukolsky, S. A., Vetterling, W. T. & Flannery, B. P. (1992). *Numerical Recipes in C. The Art of Scientific Computing.* Cambridge University Press.
Rowicka, M., Kudlicki, A. & Otwinowski, Z. (2002). *Acta Cryst.* A**58**, 574–579.
Rowicka, M., Kudlicki, A. & Otwinowski, Z. (2003*a*). *Acta Cryst.* A**59**, 172–182.
Rowicka, M., Kudlicki, A. & Otwinowski, Z. (2003*b*). *Acta Cryst.* A**59**, 183–192.
Rowicka, M., Kudlicki, A. & Otwinowski, Z. (2004*a*). In preparation.
Rowicka, M., Kudlicki, A. & Otwinowski, Z. (2004*b*). *Acta Cryst. A*. Submitted.
Tolimieri, R., An, M. & Lu, C. (1997). *Mathematics of Multi-dimensional Fourier Transform Algorithms.* New York: Springer-Verlag.